Cancer Cell
Article

Chemical Genomics Identifies Small-Molecule *MCL1* Repressors and BCL-xL as a Predictor of MCL1 Dependency

Guo Wei,[1,2,5] Adam A. Margolin,[1,5,6] Leila Haery,[1] Emily Brown,[1] Lisa Cucolo,[1] Bina Julian,[1] Shyemaa Shehata,[3] Andrew L. Kung,[2] Rameen Beroukhim,[1,3] and Todd R. Golub[1,2,4,*]
[1]Cancer Program, The Broad Institute of the Massachusetts Institute of Technology and Harvard University, Cambridge, MA 02142, USA
[2]Department of Pediatric Oncology
[3]Department of Medical Oncology
[4]Howard Hughes Medical Institute
Dana-Farber Cancer Institute, Harvard Medical School, Boston, MA 02115, USA
[5]These authors contributed equally to this work
[6]Present address: Sage Bionetworks, 1100 Fairview Avenue North, Seattle, WA 98109, USA
*Correspondence: golub@broadinstitute.org
DOI 10.1016/j.ccr.2012.02.028

SUMMARY

MCL1, **which encodes the antiapoptotic protein MCL1, is among the most frequently amplified genes in human cancer. A chemical genomic screen identified compounds, including anthracyclines, that decreased *MCL1* expression. Genomic profiling indicated that these compounds were global transcriptional repressors that preferentially affect *MCL1* due to its short mRNA half-life. Transcriptional repressors and *MCL1* shRNAs induced apoptosis in the same cancer cell lines and could be rescued by physiological levels of ectopic *MCL1* expression. Repression of MCL1 released the proapoptotic protein BAK from MCL1, and *Bak* deficiency conferred resistance to transcriptional repressors. A computational model, validated in vivo, indicated that high *BCL-xL* expression confers resistance to *MCL1* repression, thereby identifying a patient-selection strategy for the clinical development of MCL1 inhibitors.**

INTRODUCTION

Inhibition of apoptosis is a critical step in the pathogenesis of cancers, and is a major barrier to effective treatment (Adams and Cory, 2007; Danial and Korsmeyer, 2004). It is now thought that one or more components of the apoptosis pathway are dysregulated in all cancers (Hanahan and Weinberg, 2011), either by genetic mutation of the genes encoding these proteins (e.g., point mutations, copy-number abnormalities, or chromosomal translocation) or by other mechanisms (e.g., epigenetic mechanisms or upstream oncogenic mutations). Despite this central importance in the development and maintenance of cancer, few apoptosis-targeted therapeutics have reached clinical evaluation.

Of particular importance is the BCL2 family of proteins. Highly conserved from worm to human, these proteins control the activation of downstream caspases, which are the major effectors of apoptosis. The BCL2 family can be divided into three main subclasses, defined in part by the homology shared within four conserved regions termed BCL2 homology (BH) domains (Adams and Cory, 2007; Danial and Korsmeyer, 2004). The "multidomain" proapoptotic members BAX and BAK possess BH1–BH3 domains, and together constitute a requisite gateway to the intrinsic apoptosis pathway (Lindsten et al., 2000; Wei et al., 2001). In contrast, the proapoptotic proteins, such as BIM, PUMA, and NOXA, share homology only within the BH3 amphipathic α-helical death domain, prompting the title "BH3-only." Antiapoptotic family members such as BCL2, BCL-xL, and MCL1 show conservation in all four BH domains. The BH1, BH2, and BH3 domains of these proteins are in close proximity, and create a hydrophobic pocket that can accommodate the BH3 domain of a

Significance

Human tumors effectively escape cell death by activating antiapoptotic mechanisms, one of which is amplification of *MCL1*. We describe here a chemical genomic approach to the discovery of repressors of *MCL1* expression. We also identify high *BCL-xL* expression as a primary resistance mechanism to MCL1 inhibition, including resistance to anthracyclines, which we show act at least in part through an MCL1-inhibitory mechanism.

proapoptotic member (Danial and Korsmeyer, 2004; Petros et al., 2004).

Despite overwhelming genetic and functional evidence implicating the BCL2-family proteins as therapeutic targets, effective therapeutic inhibitors of these proteins have been difficult to develop. Elegant NMR-based structural biology efforts led to development of the small-molecule BCL2/BCL-xL inhibitor ABT-737 (Oltersdorf et al., 2005) and its analog ABT-263, now in early clinical trials (Tse et al., 2008). Although it is expected that ABT-263 or related compounds will have clinical activity in BCL2- or BCL-xL-dependent tumors, it is clear that many tumors do not depend on these proteins but rather rely on other antiapoptotic factors such as MCL1 (Lin et al., 2007; van Delft et al., 2006).

MCL1 has only recently been recognized as an important therapeutic target in cancer. *MCL1* is highly expressed in a variety of human cancers (Krajewska et al., 1996a, 1996b). Its expression has been linked to tumor development (Zhou et al., 2001) and resistance to anticancer therapies. For example, overexpression of MCL1 is a major resistance mechanism for the experimental BCL2/BCL-xL inhibitor ABT-737 (Chen et al., 2007; Keuling et al., 2009; van Delft et al., 2006), and MCL1 has been similarly implicated in the resistance of non-BCL2-family-targeted therapy (Wei et al., 2006). Importantly, we recently reported that amplification of the *MCL1* locus is one of the most frequent somatic genetic events in human cancer, further pointing to its centrality in the pathogenesis of malignancy (Beroukhim et al., 2010). Although the development of MCL1 inhibitors has been of considerable interest, no such inhibitors have yet reached the clinic. A particularly promising strategy, however, was recently reported by Walensky and colleagues, whereby "stapled" helical MCL1 BH3 peptides function as effective MCL1 inhibitors in preclinical models (Stewart et al., 2010). Whether such stapled peptides will make for effective clinical therapeutics remains to be established. Furthermore, no biomarkers for patient selection have been discovered for MCL1 inhibitors. Therefore, we used a chemical genomic strategy to identify MCL1-downregulating small molecules and to discover biomarkers of MCL1 dependency.

RESULTS

Gene-Expression-Based High-Throughput Screen Identifies Small Molecules Repressing MCL1 Expression

MCL1 is frequently amplified in human cancers (Beroukhim et al., 2010), and is highly expressed across a panel of 729 human cancer cell lines (see Figure S1A available online). We hypothesized that it might be possible to discover small molecules that decrease *MCL1* expression, thereby activating the apoptosis cascade in *MCL1*-dependent tumors. We therefore developed an assay to profile the mRNA levels of *MCL1* and 48 other apoptosis-related genes using the Luminex bead-based method (Hieronymus et al., 2006; Peck et al., 2006) (Figure 1A; Table S1). We profiled many apoptosis-related genes in addition to *MCL1* in order to identify compounds that preferentially repress *MCL1* while preserving expression of the proapoptotic factors.

We carried out a pilot screen using MCF7 breast cancer cells treated with 2,922 small-molecule compounds, including 530 FDA-approved drugs. We used MCF7 cells, which are deficient in caspase-3, to avoid identifying compounds that repress *MCL1* expression through feedback apoptosis mechanisms. We also performed the assay at an early time point (8 hr post-treatment) for this reason. We counterscreened against compounds that caused significant cell death at 8 hr using a lactate dehydrogenase viability assay, reasoning that such compounds must not be acting by classical apoptosis-inducing mechanisms.

Twenty-four compounds (0.8%) decreased *MCL1* expression at least 2-fold (Figure 1B). All 24 compounds reduced *MCL1* expression more than any of the other 48 apoptosis-related genes assayed, suggesting at least some degree of preferential activity against *MCL1*. We selected 14 commercially available compounds for further testing. Seven of these exhibited significant dose-related repression of *MCL1* expression. The seven compounds included the natural product triptolide, the transcription inhibitors 5,6-dichlorobenzimidazole riboside (DRB) and actinomycin D, the kinase inhibitor 5-iodotubercidin, and the anthracyclines doxorubicin, daunorubicin, and epirubicin. Despite having distinct reported mechanisms of action (Table S2), treatment with these compounds resulted in decreased MCL1 expression in multiple cell lines, suggesting a common mechanism of *MCL1* repression across cancer types (Figure S1B).

Small Molecules that Repress MCL1 Share Transcriptional Profiles

We compared genome-wide expression profiles of cells following treatment with candidate compounds to determine whether they shared a common mechanism of action. We performed genome-wide gene-expression profiling in MCF7 cells following treatment with triptolide and actinomycin D. The expression changes induced by triptolide and actinomycin D were highly similar (R^2 = 0.85), suggesting that, like actinomycin D, triptolide likely functions as a transcriptional inhibitor (Figure 1C). Consistent with this observation, triptolide was recently reported to bind to XPB, a subunit of TFIIH (Titov et al., 2011), and inhibit phosphorylation of the C-terminal tail of RNA polymerase II, which results in transcriptional inhibition (Leuenroth and Crews, 2008).

Using the Connectivity Map database containing expression profiles of 1,366 compounds (http://www.broadinstitute.org/cmap) (Lamb et al., 2006), the triptolide-induced profile showed a high degree of similarity to both doxorubicin and daunorubicin (ranked 1 and 2 of 1,366, respectively, using Spearman correlation) (Figure 1D). The anticancer effect of anthracyclines has long been attributed to inhibition of DNA topoisomerase II (Desmedt et al., 2011; Moretti et al., 2009). However, the DNA topoisomerase II inhibitor etoposide induced a transcriptional profile distinct from that induced by triptolide (Figure 1D). Taken together, these results strongly suggest that the compounds that emerged from our *MCL1*-repression screen, including the anthracyclines, function as global transcriptional repressors. We therefore refer to them as transcriptional repressor (TR) compounds.

Strikingly, the TR compounds showed dramatic preferential activity against *MCL1* compared to the rest of the transcriptome. For example, *MCL1* was in the top 0.05 percentile of

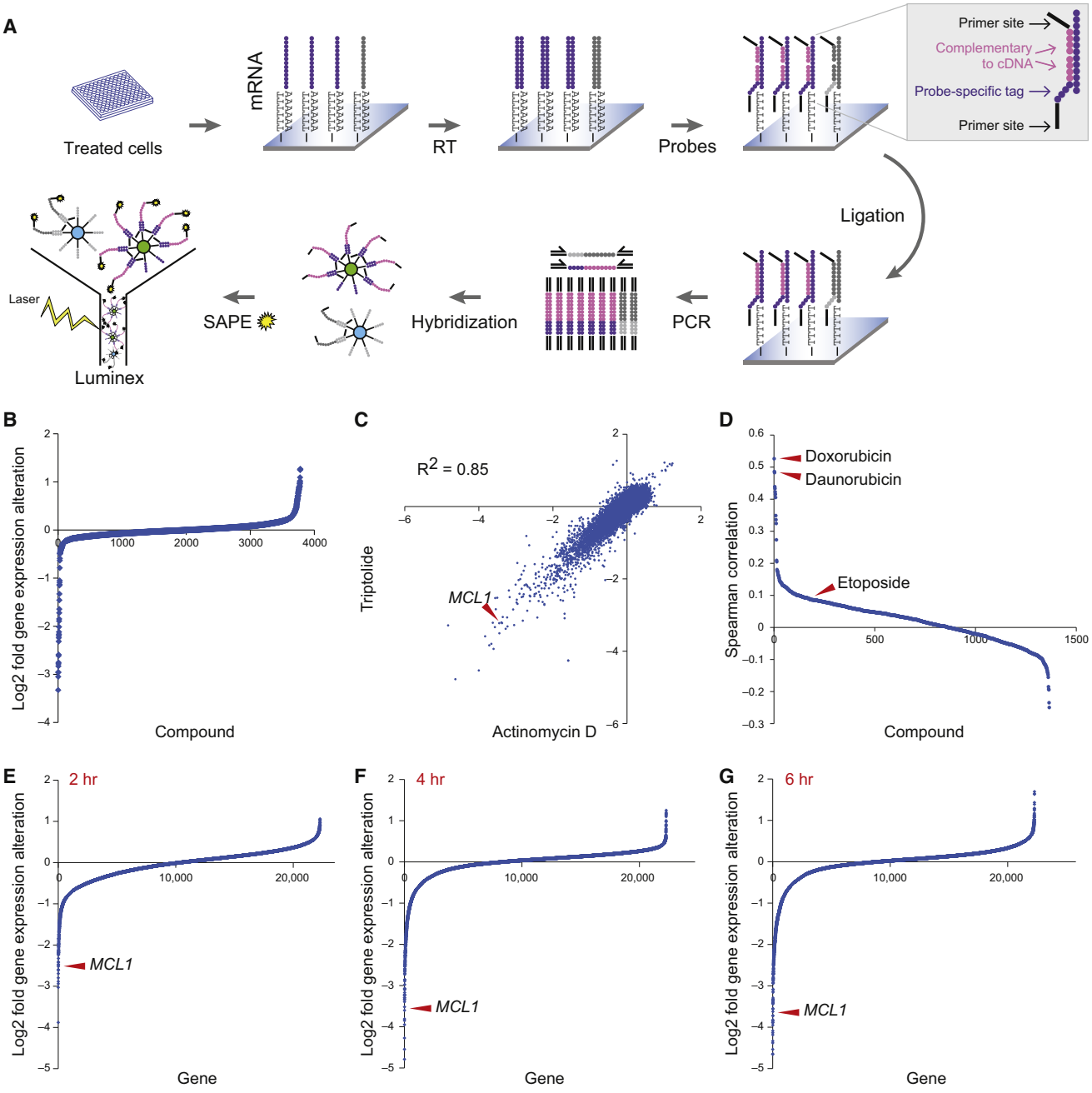

Figure 1. Bead-Based High-Throughput Gene-Expression Screening Identified *MCL1* Repression by Transcriptional Inhibitor Compounds

(A) Illustration of screening procedure. mRNA levels of *MCL1* and 48 other apoptotic genes were measured in MCF7 cells 8 hr after treatment with 2,922 small molecules.

(B) *MCL1* expression modulation by 2,922 compounds. Compounds and DMSO controls were sorted by *MCL1* expression repression. The y axis displays log2 gene-expression fold change.

(C) Gene-expression profiling by Affymetrix microarrays of MCF7 cells with triptolide (500 nM) and actinomycin D (2.5 μM) for 4 hr. Both the x and y axes display log2 gene-expression fold alteration.

(D) The 1,317 compounds used to treat MCF7 cells in the Connectivity Map are displayed in descending order of their correlation with triptolide (calculated as the Spearman rank correlation of the differential gene expression across the Affymetrix U133A chip).

(E–G) Gene-expression repression by triptolide at 2 hr (E), 4 hr (F), and 6 hr (G). The genes are ranked by the extent of repression. The y axis displays log2 gene-expression fold alteration. Arrowheads indicate *MCL1*.

See also Figure S1 and Tables S1 and S2.

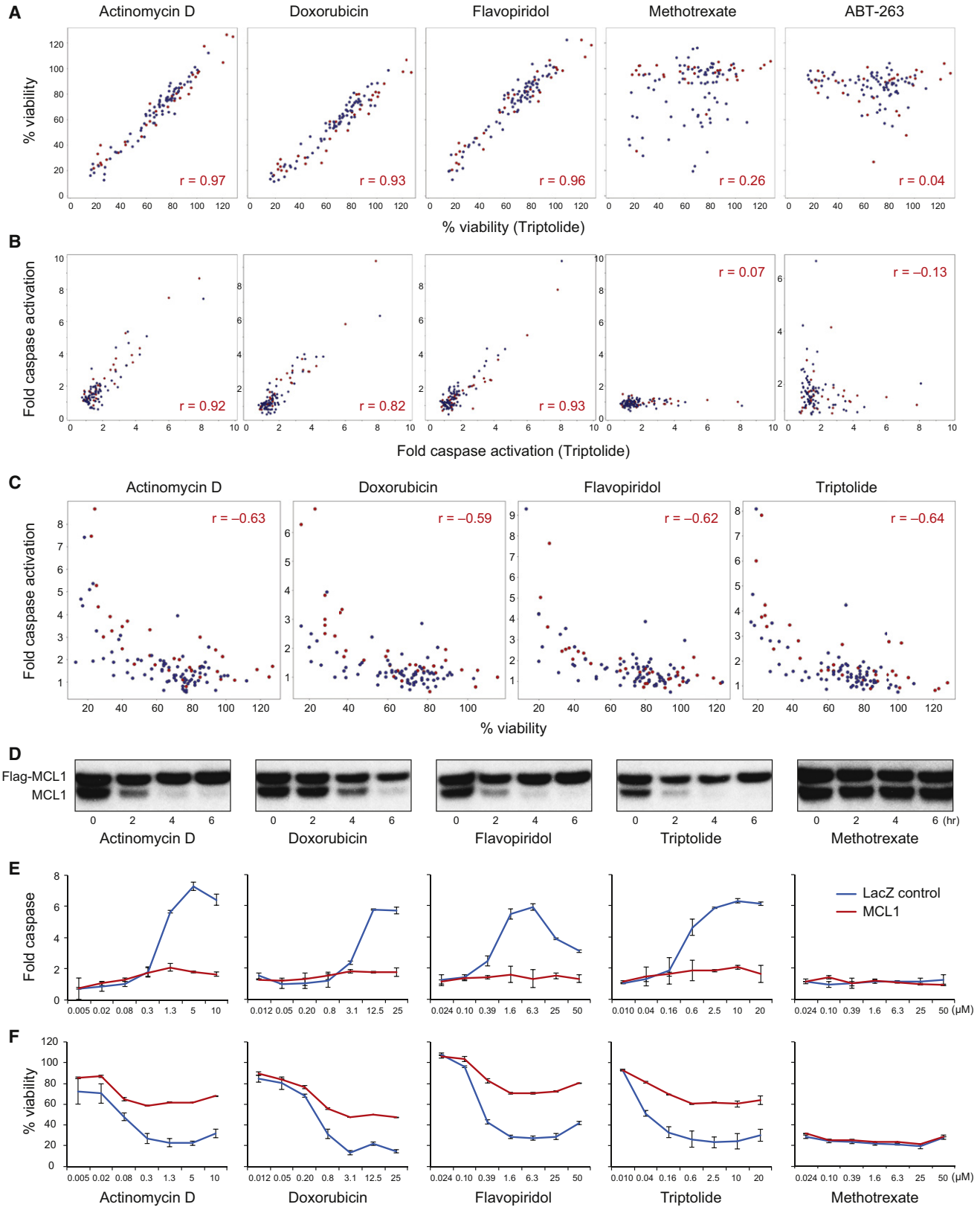
A
Actinomycin D
Doxorubicin
Flavopiridol
Methotrexate
ABT-263
% viability
r = 0.97
r = 0.93
r = 0.96
r = 0.26
r = 0.04
% viability (Triptolide)
B
Fold caspase activation
r = 0.92
r = 0.82
r = 0.93
r = 0.07
r = –0.13
Fold caspase activation (Triptolide)
C
Actinomycin D
Doxorubicin
Flavopiridol
Triptolide
Fold caspase activation
r = –0.63
r = –0.59
r = –0.62
r = –0.64
% viability
D
Flag-MCL1
MCL1
Actinomycin D
Doxorubicin
Flavopiridol
Triptolide
Methotrexate
6 (hr)
E
Fold caspase
LacZ control
MCL1
50 (μM)
F
% viability
Actinomycin D
Doxorubicin
Flavopiridol
Triptolide
Methotrexate
50 (μM)

triptolide-repressed genes (Figures 1E–1G), and the *MCL1* transcript was repressed more than 5-fold within 2 hr of treatment (Figure 1E). On the contrary, none of the other BCL2-family genes were repressed more than 2-fold. Consistent with the reported short half-life of MCL1 protein (30 min) (Adams and Cooper, 2007), inhibition of *MCL1* mRNA caused a rapid decrease in MCL1 protein levels that occurred prior to poly(ADP ribose) polymerase (PARP) cleavage, a marker for caspase activation (Figure S1C).

TR Compounds Share a Pattern of Cell Killing and Can Be Rescued by Physiologically Relevant Levels of MCL1

Based on the shared mechanisms suggested above, we hypothesized that if *MCL1* repression is a biologically relevant target of TR compounds, then these compounds should induce apoptosis in the same cancer cell lines. We therefore measured caspase activation and cell viability of 74 non-small-cell lung cancer (NSCLC) and 33 breast cancer cell lines following treatment with actinomycin D, doxorubicin, triptolide, and flavopiridol. Flavopiridol has previously been reported to repress *MCL1* expression via inhibition of CDK9 (Chen et al., 2005).

Responses to the TR compounds were highly correlated when measured both by caspase activation and cell viability (Pearson $r > 0.82$ and 0.93, respectively, when compared to triptolide) (Figures 2A and 2B). As expected, cell viability was highly correlated with caspase activation for each TR compound (Figure 2C; Pearson $r > 0.59$), indicating that the TR compounds impair cell viability via apoptosis. By contrast, compounds that kill cells via different mechanisms, such as methotrexate and etoposide, demonstrated different patterns of cytotoxicity (Figures 2A and 2B; Figure S2A). Despite the fact that TR compounds repress the expression of many genes, ectopic expression of physiological levels of MCL1 rescued cells from TR-compound treatment (Figures 2D–2F). In contrast, ectopic expression of *MCL1* had no such rescue effect for other classes of compounds, such as methotrexate (Figures 2D–2F).

If TRs block global transcription, we hypothesized that combination treatment with TR compounds would counteract the effects of compounds that kill cells by inducing the expression of proapoptotic proteins. The proteasome inhibitor bortezomib induces apoptosis through the induction of the proapoptotic protein NOXA (Gomez-Bougie et al., 2007; Voortman et al., 2007). As predicted, treatment with the TR compounds doxorubicin, actinomycin D, or triptolide rescued cells from the apoptotic effects of bortezomib, whereas treatment with the non-TR compound etoposide had no effect (Figures S2B–S2F). Similarly, the TR compounds were able to rescue cells from the histone deacetylase (HDAC) inhibitor vorinostat (Figure S2G), which kills cells via the induction of the proapoptotic proteins BMF and NOXA (Wiegmans et al., 2011).

MCL1 Knockdown Phenocopies TR Compounds

In order to determine whether *MCL1* repression explains the activity of TR compounds, we tested whether their effects could be phenocopied by knockdown of *MCL1*. We treated 17 breast cancer and 16 NSCLC cell lines representing different levels of sensitivity to TR compounds with each of the five most effective shRNAs selected from a library of 60 anti-*MCL1* shRNAs (Figure 3A). The response to the five *MCL1* shRNAs was highly correlated ($R^2 > 0.64$ for breast cell lines and $R^2 > 0.55$ for NSCLC cell lines) (Figure 3B). Ectopic expression of *MCL1* with a heterologous 3′ UTR at physiologically relevant levels was able to rescue cells from the two *MCL1* shRNAs targeting the 3′ UTR of *MCL1* but not the three *MCL1* shRNAs targeting the coding region of *MCL1* (Figure 3C), indicating that their cellular effects are most likely due to *MCL1* repression as opposed to off-target effects.

In addition, we generated shRNAs against *BCL-xL* to test whether *MCL1*-dependent cells were sensitive to knockdown of other antiapoptotic genes. The responses to the five most effective *BCL-xL* shRNAs (out of the 24 shRNAs tested) were highly correlated (Figures 3D and 3E; Figure S3A), but these responses did not correlate with the response to the *MCL1* shRNAs ($R^2 = 0.002$) (Figure 3F; Figure S3B).

Impaired viability induced by doxorubicin was strongly correlated with the effects of *MCL1* shRNAs [$R^2 = 0.80$ for breast cancer cells (Figure 3G) and $R^2 = 0.74$ for NSCLC cells]. Conversely, doxorubicin sensitivity did not correlate with the effects of shRNAs targeting *BCL-xL* ($R^2 = 0.0001$ for breast cancer cell lines) (Figure 3H). Furthermore, doxorubicin did not induce additional significant cell death after *MCL1* knockdown, consistent with *MCL1* repression being a major effector of doxorubicin action (Figures 3I and 3J). Triptolide yielded similar results, suggesting that this is a general property of TR compounds (Figure S3C). Taken together, these results further support the notion that a subset of tumor cells is dependent upon MCL1 for survival, and that TR compounds act largely via *MCL1* repression.

Discovering Predictive Biomarkers of MCL1 Essentiality

We next sought to discover biomarkers that are predictive of *MCL1* essentiality by comparing TR-compound sensitivities with genomic data. Such biomarkers would prove useful for the prediction of sensitivity to any present or future MCL1

Figure 2. TR Compounds Shared a Pattern of Cell Killing

(A and B) Seventy-four NSCLC (blue dots) and 33 breast cancer (red dots) cell lines were treated with small molecules. The effect of triptolide (x axis) is compared with the effect of other compounds (y axis), measured both by cell viability after 24 hr of treatment (A) and fold-caspase-3 activation after 6 hr of treatment (B). Concentrations of the compounds for the displayed data were actinomycin D (1.25 μM), doxorubicin (12.5 μM), flavopiridol (6.25 μM), methotrexate (6.25 μM), ABT-263 (6.25 μM), and triptolide (2.5 μM).

(C) Correlation between cell viability and caspase activation.

(D) Expression levels of endogenous MCL1 and FLAG-MCL1 in HMC-1-8 cells after treatment with the indicated compounds were evaluated by western blot. For each panel, cells were treated with the compound for 0, 2, 4, and 6 hr (left to right for each compound).

(E and F) Ectopic expression of physiological levels of FLAG-MCL1 rescued HMC-1-8 cells from TR compounds but not methotrexate, as measured by caspase activation at 6 hr (E) and cell viability at 24 hr (F). Error bars indicate standard deviation of duplicate measurements.

See also Figure S2.

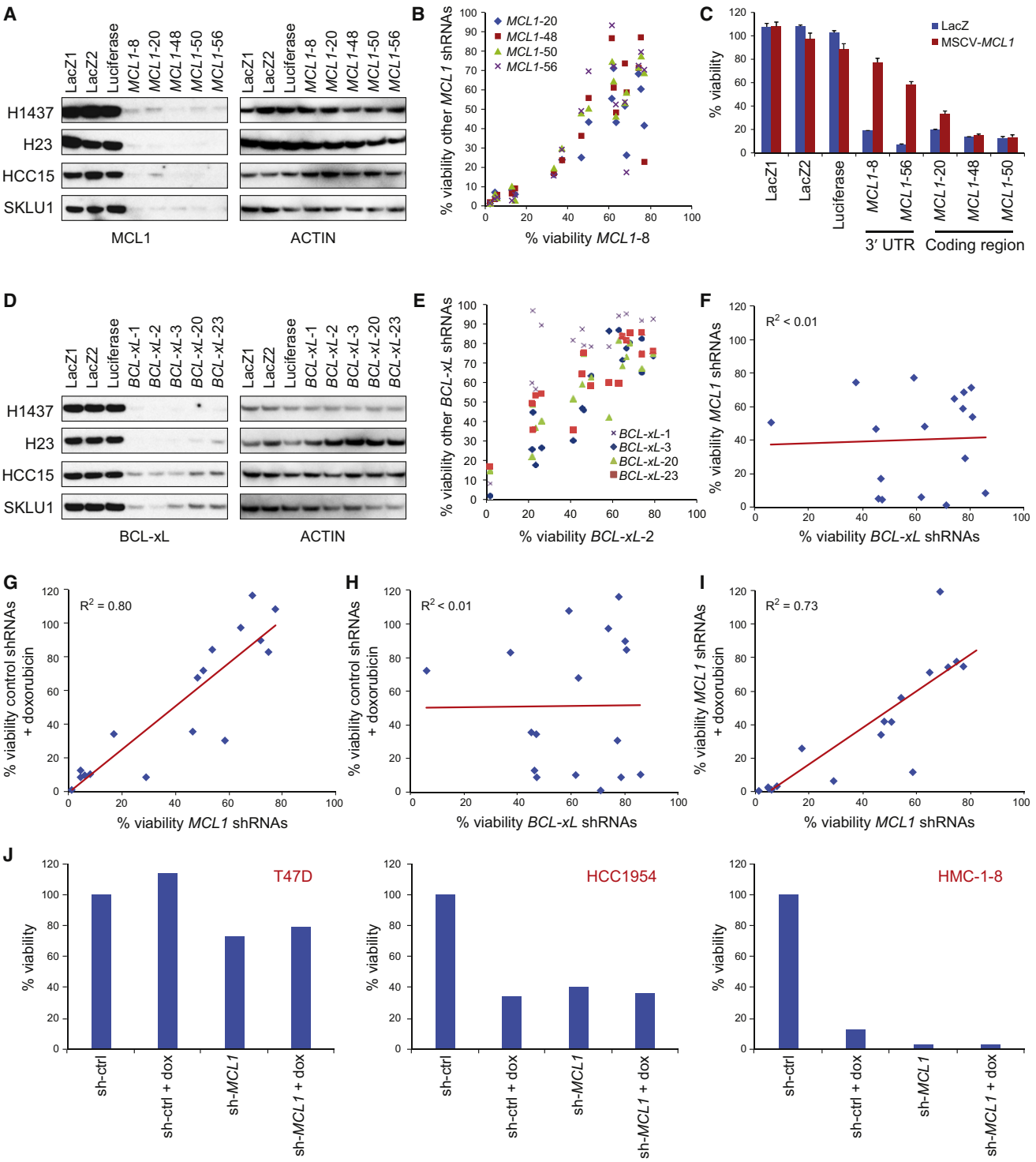

Figure 3. *MCL1* Knockdown Phenocopied TR Compounds

(A) Knockdown efficiency of the five best *MCL1* shRNAs as determined by western blot.

(B) Effects of one shRNA (*MCL1*-8) on cell viability are plotted on the x axis against the effects of the other four *MCL1* shRNAs on the y axis. Data were measured from 17 breast cancer cell lines.

(C) Effect of expressing physiological levels of FLAG-tagged MCL1 on apoptosis induced by *MCL1* shRNAs targeting the 3′ UTR of *MCL1* (*MCL1*-8 and *MCL1*-56) or targeting the coding region of *MCL1* (*MCL1*-20, *MCL1*-48, and *MCL1*-50) in HMC-1-8 cells. Error bars indicate standard deviation of duplicate measurements.

(D) Five *BCL-xL* shRNAs effectively knocked down BCL-xL expression. H1437 and H23 cells had longer exposure time than HCC15 and SKLU1 cells for western blots to show the shRNA effects.

inhibitors. We developed an analytical method to infer groups of compounds that induce sensitivity in similar cancer genetic subtypes and infer predictive biomarkers of sensitivity to each compound group. Briefly, the method uses an expectation-maximization algorithm and iterates until convergence between clustering groups of compounds based on the similarity of their response profiles, and uses an elastic net algorithm to infer a predictive model for each group based on its genetic features (Lee et al., 2009). The method further employs a bootstrapping procedure to obtain a parsimonious model containing only robustly predictive features (Figure 4A; see Supplemental Experimental Procedures for details).

We examined the genetic features (copy number and expression data for >18,000 genes, and mutation data for 34 genes) across 72 cell lines for which we had TR-compound sensitivity measurements. To ensure that our predicted biomarkers were specific to sensitivity induced by the TR compounds, we also performed dose-response measurements on 37 additional control compounds (Table S2). The algorithm identified a cluster of compounds consisting of all of the TR compounds (actinomycin D, doxorubicin, flavopiridol, and triptolide), as well as three additional compounds (puromycin, emetine, and anisomycin) that function as global repressors of protein translation (Figure 4B). Similar to *MCL1* mRNA, the extremely short half-life of MCL1 protein likely explains the selective effects of protein translation inhibitors on MCL1 activity.

The predictive model of sensitivity to the group of transcriptional and translational repressors contained only a single feature, corresponding to mRNA expression of *BCL-xL*. Specifically, low expression of *BCL-xL* was associated with sensitivity, and high expression of *BCL-xL* was associated with resistance to compounds that repress *MCL1* expression. The half-life of BCL-xL protein is much longer than that of MCL1 (Figure S1C), consistent with its ability to prevent apoptosis induced by transcriptional and translational inhibitors. Also consistent with this observation, sensitivity to *MCL1* shRNAs anticorrelated with *BCL-xL* mRNA levels in the 17 breast cancer cell lines ($R^2 = 0.57$) (Figure 4C).

We next sought to derive a computational model for the causal interactions that explain how *MCL1* and *BCL-xL* influence sensitivity to TR compounds. We applied the ARACNE reverse-engineering algorithm (Basso et al., 2005; Margolin et al., 2006), which is designed to deconvolute direct and indirect interactions among a set of covariates, and derived a network of direct interactions among variables corresponding to gene expression and copy number of *MCL1* and *BCL-xL* and sensitivity to TR compounds. We used as input to the algorithm a matrix of values across the panel of 72 cell lines, corresponding to normalized expression and copy number of *MCL1* and *BCL-xL*, as well as sensitivity to the TR compounds, computed as the average of normalized IC_{50} values across all TR compounds. This approach yielded a model in which expression of *BCL-xL* was indeed the direct predictor of sensitivity to TRs (Figure 4D). As expected, gene expression of *BCL-xL* and *MCL1* was directly influenced by the copy number of the respective genes (Figures 4E and 4F). Interestingly, the model indicated an epistatic relationship between *MCL1* copy number and *BCL-xL* expression. *MCL1* copy number was negatively correlated with *BCL-xL* expression (Figure 4G), suggesting that *MCL1* amplification may decrease the selective pressure requiring *BCL-xL* for inhibition of apoptosis.

Sequestration of Proapoptotic Proteins by MCL1 and BCL-xL

The above data suggested that breast and lung cancer cells with low expression of BCL-xL rely on MCL1 to sequester proapoptotic proteins. Upon repression of MCL1 protein levels, proapoptotic proteins might be released from MCL1 and cause downstream caspase activation and apoptosis. BIM binds to all antiapoptotic proteins (Mérino et al., 2011). In a panel of 19 NSCLC cell lines, in cells expressing low levels of BCL-xL, depletion of MCL1 by immunoprecipitation resulted in depleting nearly the entirety of BIM (Figures 5A and 5B). In contrast, in cells expressing high levels of BCL-xL, only a small fraction of BIM was sequestered by MCL1 (Figures 5A and 5B). Furthermore, when BCL-xL was overexpressed in cells that normally have low levels of BCL-xL, the fraction of BIM bound by MCL1 decreased significantly (Figure 5C). These experiments demonstrate a shuttling of BIM sequestration between MCL1 and BCL-xL, depending on their relative expression levels. To explore whether the release of BIM from MCL1 explains the apoptotic effect of MCL1-repressing TR compounds, we repeated the MCL1-BIM coimmunoprecipitation experiments under conditions of TR treatment. Surprisingly, despite the TR compounds triptolide or flavopiridol significantly reducing MCL1 levels, the majority of BIM protein remained bound to the residual MCL1 (Figures S4A and S4B). In addition, *BIM* knockdown by shRNA did not abrogate the sensitivity to TR compounds (Figures S7C–S7G), although we cannot exclude the possibility that more complete BIM knockdown might have a more dramatic effect.

Because BIM seemed unlikely to be the principal proapoptotic mediator of MCL1 repression, we considered other candidate proteins. MCL1 coimmunoprecipitation experiments showed that whereas the majority of PUMA, BAK, and BAX proteins were not bound by MCL1 (Figure 5A; Figure S4A), significant amounts of PUMA and BAK were pulled down by MCL1, and overexpression of BCL-xL disrupted this interaction (Figures 5C and 5D). MCL1-bound PUMA decreased after triptolide-mediated MCL1 repression, but this result is best explained by triptolide's concomitant repression of PUMA expression (Figure 5D). To test the possibility that BAK release from MCL1

(E) Effects of one shRNA (*BCL-xL-2*) on cell viability are plotted on the x axis against the effects of the other four *BCL-xL* shRNAs on the y axis. Data were measured from 17 breast cancer cell lines.
(F–I) Effects of *MCL1* shRNAs (G and I) or *BCL-xL* shRNAs (F and H) on cell viability plotted on the x axis against sensitivity to *MCL1* shRNAs (F), doxorubicin (G and H), or *MCL1* shRNAs + doxorubicin (I) plotted on the y axis in 17 breast cancer cell lines. Cells were infected with viruses carrying shRNAs for *MCL1* or *BCL-xL* for 3 days, or 2 days followed by treatment with 5 μM doxorubicin for an additional 24 hr (median of five *MCL1* shRNAs or *BCL-xL* shRNAs, as indicated).
(J) Examples of cell lines that were resistant (T47D), partially sensitive (HCC1954), or sensitive (HMC-1-8) to *MCL1* inhibition. Dox, doxorubicin.
See also Figure S3.

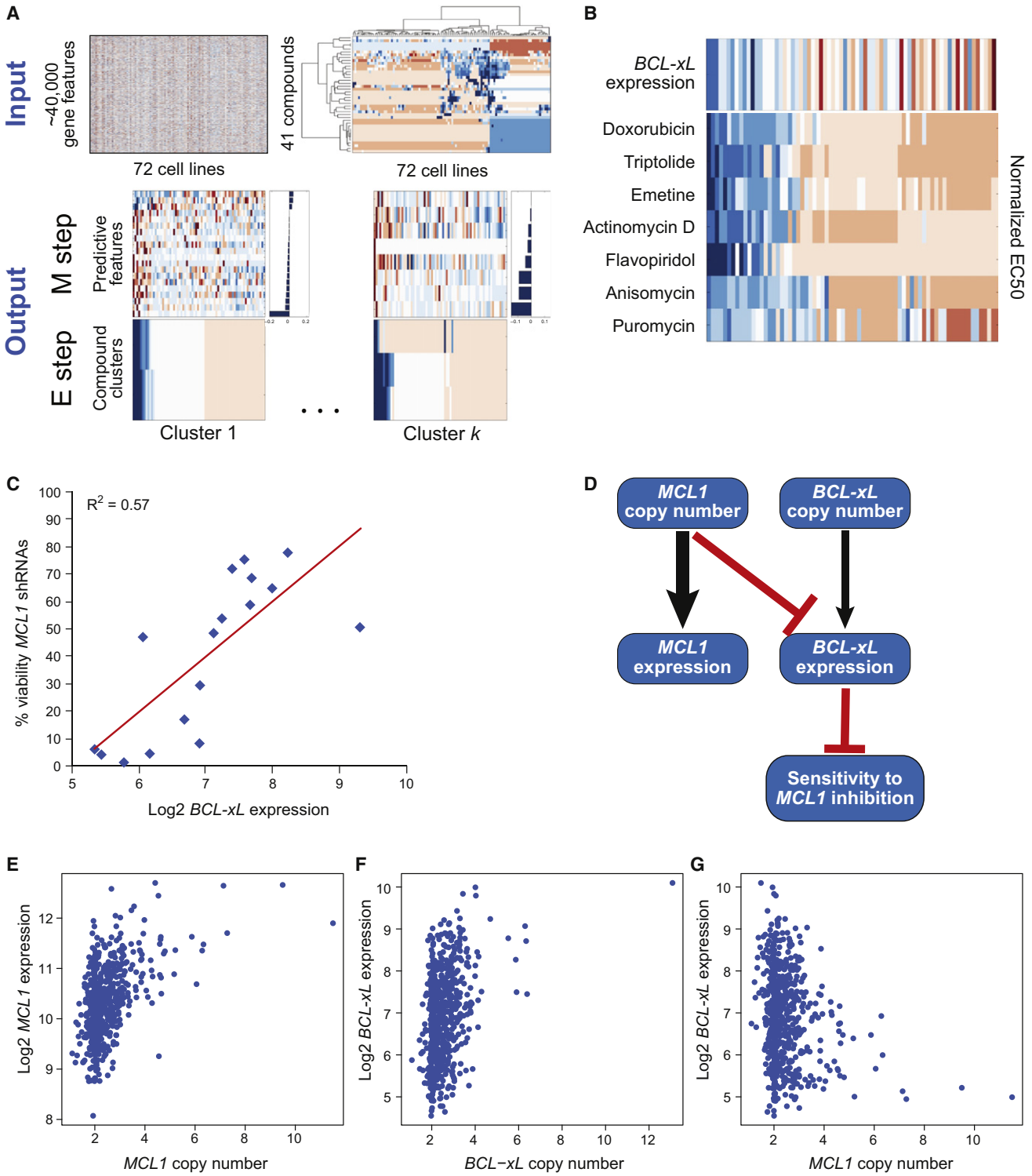

Figure 4. Unbiased Computational Analysis Identified TR Compound Sensitivity Predicted by Low Expression of *BCL-xL*

(A) Schematic of biomarker discovery algorithm (see Supplemental Experimental Procedures for details).

(B) *BCL-xL* expression as a predictive biomarker of TR-compound sensitivity. The expectation-maximization algorithm identified one cluster that contained all of the TR compounds (bottom panel; blue indicates drug sensitivity, red indicates resistance), coupled to a single predictive feature, *BCL-xL* RNA expression (top panel; blue indicates low level of expression, red indicates high expression).

(C) Correlation between expression level of *BCL-xL* (x axis) and cell viability upon *MCL1* knockdown (y axis), represented as the percent viability relative to control shRNAs, averaged over two replicates treated for 3 days with five different shRNA constructs targeting *MCL1* across a panel of 17 breast cancer cell lines.

explains the TR effect, we used *Bak*$^{-/-}$ MEFs to determine contribution of Bak in TR compound-induced apoptosis. *Bak* deletion nearly completely rescued cells from TRs but did not protect cells from the non-TR compound trichostatin A (Figures 5E–5H). BAX and BAK are both multidomain proapoptotic BCL2-family proteins. However, BAK proved unique in that we did not detect MCL1-BAX interaction in coimmunoprecipitation experiments (Figures 5C and 5D), and *Bax*$^{-/-}$ cells were not rescued from TR compounds (Figures 5E–5G). Taken together, our data suggest that MCL1 protects cells from cell death at least in part through sequestration of BAK, and this sequestration is diminished with TR compound-mediated *MCL1* repression.

BCL-xL Predicts MCL1 Dependency In Vivo

An important question in developing biomarkers of MCL1 dependency is whether resistance mechanisms observed in vitro hold in vivo, where tumor-microenvironment interactions are known to modulate apoptotic mechanisms (Bewry et al., 2008; Buggins et al., 2010). We therefore examined the in vivo response of two NSCLC cell lines grown as xenografts in NOD-SCID mice. H1437 cancer cells express low levels of *BCL-xL* and are sensitive to triptolide (as a prototype *MCL1* repressor) in vitro. HCC15 cells, in contrast, express high levels of *BCL-xL* and are triptolide resistant in vitro. This pattern of sensitivity persisted in vivo. Triptolide significantly attenuated the growth of the H1437 NSCLC cancer model (Figures 6A and 6B). By contrast, in the HCC15 xenograft model, triptolide did not significantly affect tumor volume or survival of the mice (Figures 6C and 6D). Western blotting of whole-tumor lysates demonstrated that treatment with triptolide decreased MCL1 protein abundance and increased PARP cleavage in the H1437 xenograft model (Figure 6E), indicating that triptolide repressed MCL1 expression and induced apoptosis in vivo.

Our model predicts that patients with high levels of *BCL-xL* expression are resistant to TRs. To test this hypothesis, we investigated the relationship between *BCL-xL* gene expression and clinical response to neoadjuvant treatment with the anthracycline epirubicin in 114 estrogen receptor (ER)-negative breast cancer patients for which it was determined whether a complete pathological response (pCR) was achieved (Desmedt et al., 2011). *BCL-xL* showed significant differential expression between patients who achieved pCR and those who did not (Figure 6F). As previously reported, expression of topoisomerase 2A (TOP2A) did not correlate with response to epirubicin (Figure S5), consistent with our finding that anthracyclines kill tumor cells via a transcriptional repressive mechanism rather than via a topoisomerase-inhibitory mechanism as has been generally assumed.

BCL-xL Is a Functional Determinant of MCL1 Dependency

We next investigated whether *BCL-xL* was simply a marker of MCL1 dependency or whether it was a functional determinant of response. Overexpression of *BCL-xL* in MCL1-dependent lines protected them from apoptosis induced by *MCL1* shRNAs or TR compounds (Figures 7A–7C) but not by other cytotoxic agents such as methotrexate (Figures 7B and 7C), suggesting a specific effect for TR compounds. Conversely, *BCL-xL* knockdown conferred sensitivity in cell lines otherwise resistant to TR compounds. Cell lines resistant to treatment with TR compounds (using doxorubicin as a representative example) were sensitive to combined treatment with *BCL-xL* shRNAs (Figures 7D and 7G), and cell lines resistant to treatment with *MCL1* shRNAs were sensitive to combined treatment with the BCL-xL inhibitor ABT-263 (Figures 7E and 7G). The viability of cells treated with *BCL-xL* shRNAs was highly correlated with viability after treatment with the BCL-xL inhibitor ABT-263, and combined treatment of cells with ABT-263 and *BCL-xL* shRNAs did not yield synergistic effects (Figures 7F and 7G).

The above data suggest that TR compounds would exhibit a synergistic effect when used in combination with BCL-xL inhibitors. We treated a panel of 74 NSCLC cell lines with a 42-point dose-response matrix (six concentrations of triptolide or actinomycin D, and seven concentrations of ABT-263 or ABT-737). We examined the synergy between TR compounds and BCL-xL inhibitors for each cell line by computing the excess growth inhibition over the Bliss independence model for each combination of compound concentrations (Figures 8A–8C). Cell lines that were highly sensitive to TR compounds showed no evidence of synergy when treated in combination with ABT-737. Cell lines that were resistant to TR compounds and to BCL-xL inhibitors were sensitive to the combination (Figures 8A–8C).

A synergy score was computed for each combination experiment in each of the 74 NSCLC cell lines by summing the excess over Bliss independence across all dose combinations. The synergy score was averaged over the four combination experiments, performed by pairing triptolide or actinomycin D with ABT-263 or ABT-737. This synergy score was highly correlated with expression of *BCL-xL* (Figure 8D), suggesting that high expression of *BCL-xL* determines the synergistic relationship between TR compounds and BCL-xL-inhibitory compounds, and that resistance to TR compounds, caused by high expression of *BCL-xL*, can be overcome by treating in combination with BCL-xL inhibitors. Consistent with this notion, ABT-263 released BAK from BCL-xL (Figure 8E).

DISCUSSION

At an accelerating pace, the genomic characterization of human cancer is elucidating the molecular basis of the disease. Recent large-scale analyses of gene copy number in cancer demonstrated that the genes encoding the BCL2-family proteins MCL1 and BCL-xL are frequent targets of amplification. Low-level *MCL1* amplification is particularly notable, representing one of the most common copy-number abnormalities in all of

(D) The ARACNE reverse-engineering algorithm was used to identify direct interactions between sensitivity to TR compounds and *MCL1* and *BCL-xL* gene expression and gene copy number. Arrows represent inferred direct interactions, with the weight of the edge proportional to the mutual information between the corresponding nodes. Arrows indicate the presumed direction of causality (e.g., copy number to gene expression). Black lines indicate positive correlations and red lines indicate negative correlations.
(E–G) Comparisons of gene expression and copy-number values of *MCL1* and *BCL-xL* across 643 cancer cell lines. (E) *MCL1* copy number versus *MCL1* expression. (F) *BCL-xL* copy number versus *BCL-xL* expression. (G) *MCL1* copy number versus *BCL-xL* expression.

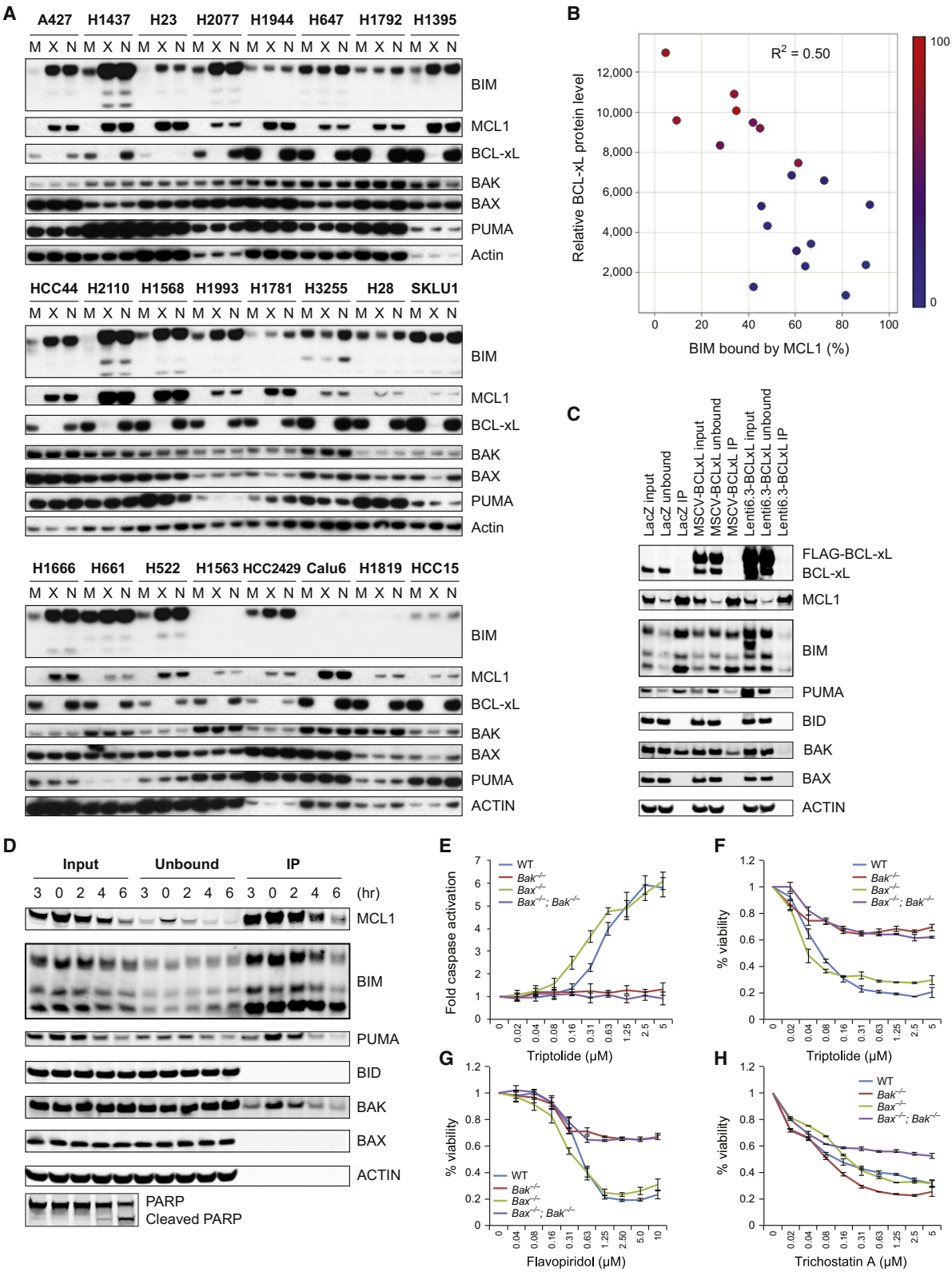

Figure 5. MCL1 Is the Major Antiapoptotic Protein in Cells with Low BCL-xL Expression

(A and B) Cell lysates of the indicated NSCLC cell lines were subjected to immunoprecipitation with an anti-MCL1 antibody (M), an anti-BCL-xL antibody (X), or no antibody control (N). The indicated proteins left in the postimmunoprecipitation fraction were detected using western blotting (A). The fraction of unbound BIM and BIM input was quantified by ImageJ software, and the color denotes cell viability after 24 hr of treatment with triptolide (B).

human cancer (Beroukhim et al., 2010). In support of a functionally important role of MCL1, numerous studies have elucidated the critical role of MCL1 in preventing tumor cell death (Warr and Shore, 2008).

Using a multiplexed Luminex bead-based assay, we screened for compounds that reduced *MCL1* expression while preserving the expression of proapoptotic genes. Although the compounds that emerged from this screen were general transcriptional repressor compounds (as opposed to specifically targeting the *MCL1* locus), they preferentially repressed *MCL1* because of the short half-life of *MCL1* mRNA and protein. Multiple lines of evidence suggest that TR compounds induce apoptosis in cancer cells primarily through repression of *MCL1* expression, including: (1) upon treatment with TR compounds, MCL1 protein levels decreased rapidly and preceded caspase activation; (2) ectopic expression of physiological levels of *MCL1* rescued cancer cells from TR compounds, despite the expression of other genes still being repressed; (3) the pattern of TR-compound sensitivity across a panel of cancer cell lines closely mirrored the pattern of sensitivity of those cell lines to *MCL1* knockdown by RNAi; (4) of over 40,000 genomic features measured, the top feature that predicted sensitivity to TR compounds was the low expression of *BCL-xL*, which shares redundant function with *MCL1*; (5) ectopic expression of *BCL-xL* rescued cancer cells from TR compounds; (6) *MCL1* repression by TR compounds resulted in the release of proapoptotic protein BAK from MCL1; and (7) *Bak* deficiency protected cells from TR compounds. These results suggest that the mechanism of cell death induced by TR compounds is best explained by *MCL1* inhibition.

This indicated that some of the widely used chemotherapeutic drugs such as anthracyclines may preferentially repress *MCL1* to induce apoptosis in tumor cells. Although the antitumor effect of anthracyclines has long been speculated to be related to the drug's inhibition of DNA topoisomerase II (Desmedt et al., 2011; Moretti et al., 2009) and an association between low TOP2A expression and anthracycline response in ER-negative breast cancer patients has been reported (Martin et al., 2011), our data suggest that their activity may be largely explained by inhibition of transcription, leading most dramatically to the repression of short-lived *MCL1* transcripts. Although it is possible that multiple mechanisms of action explain the antitumor effects of anthracyclines, at least in the experimental cancer models studied here, anthracycline gene-expression consequences most reflected transcriptional inhibition rather than DNA topoisomerase II inhibition. Furthermore, the similar pattern of sensitivity of cell lines to *MCL1* knockdown compared to anthracycline treatment is also consistent with an *MCL1*-mediated transcriptional inhibitory effect. Last, our observation that *BCL-xL* expression is predictive of resistance to *MCL1* repression both in model systems and in patients with breast cancer further strengthens the anthracycline-*MCL1* connection. We note that the concentration of doxorubicin used in our experiments approximates that observed in human tumor tissues (1.9–24.4 μM) (Rossi et al., 1987). Doxorubicin stimulates topoisomerase II-mediated DNA cleavage only at low concentrations, whereas at doses greater than ~0.4 μM, topoisomerase II-mediated DNA cleavage is lost (Tewey et al., 1984). These data therefore suggest that at clinically relevant concentrations, anthracyclines act as transcriptional repressors, as opposed to DNA-damaging agents.

The transcriptional inhibitory role of anthracyclines is also of importance when considering anthracycline-based combination therapies. The transcriptional induction of proapoptotic proteins has been reported to be crucial for the efficacy of many classes of antineoplastic agents including radiation (Jeffers et al., 2003; Villunger et al., 2003), the proteasome inhibitor bortezomib (Gomez-Bougie et al., 2007; Voortman et al., 2007), the HDAC inhibitor vorinostat (Wiegmans et al., 2011), and the kinase inhibitors imatinib (Kuroda et al., 2006) and erlotinib (Gong et al., 2007). Anthracyclines may block the induction of such proapoptotic proteins and counteract, rather than synergize with, those therapies. For example, we found that doxorubicin treatment actually rescues cancer cells from bortezomib- and vorinostat-induced killing (Figure S2). Such antagonistic actions may be preventable by adjusting the dosing schedule of combination therapies, but the results serve as a reminder that knowledge of mechanisms of action should ideally be considered in developing combination strategies.

Taken together, the results reported here elucidate a strategy for the development of MCL1 inhibitors as cancer therapeutics. The multiplexed, gene-expression-based high-throughput screening approach described here holds promise for the future discovery of specific inhibitors of *MCL1* expression and for the use of chemical genomic approaches to elucidate small-molecule mechanisms of action. The study also highlights the power of genomically characterized cell lines for the discovery of predictive biomarkers of drug response. Most immediately, the work suggests an approach to the clinical development of any MCL1 inhibitor in breast and NSCLC tumors, focusing on tumors expressing low levels of *BCL-xL* as a patient-selection strategy.

EXPERIMENTAL PROCEDURES

Cell Culture, Caspase, and Viability Assay

All human cell lines were part of the Broad-Novartis Cancer Cell Line Encyclopedia Project (http://www.broadinstitute.org/ccle/home) or gifts from

(C) HMC-1-8 cells stably expressing FLAG-BCL-xL via the MSCV retroviral vector or the Lenti6.3 lentiviral vector, or LacZ control were subjected to immunoprecipitation using an anti-MCL1 antibody. Input, unbound, and immunoprecipitation (IP) fractions were analyzed by western blotting. The IP fraction was 5-fold more concentrated than input and unbound.

(D) HMC-1-8 cells were treated with 2 μM triptolide for the indicated times and subjected to immunoprecipitation with an anti-MCL1 antibody conjugated to agarose beads, eluted with an MCL1 peptide, and western blotted for proapoptotic proteins. The IP fraction was 5-fold more concentrated than input and unbound.

(E–H) Wild-type (WT), $Bak^{-/-}$, $Bax^{-/-}$, and $Bax^{-/-}$;$Bak^{-/-}$ MEFs were treated with TR compounds triptolide (E–F) or flavopiridol (G), or non-TR compound trichostatin A (H), at the indicated concentrations for 7 hr (E, for caspase activation) or 24 hr (F–H, for viability). Error bars indicate standard deviation of duplicate measurements.

See also Figure S4.

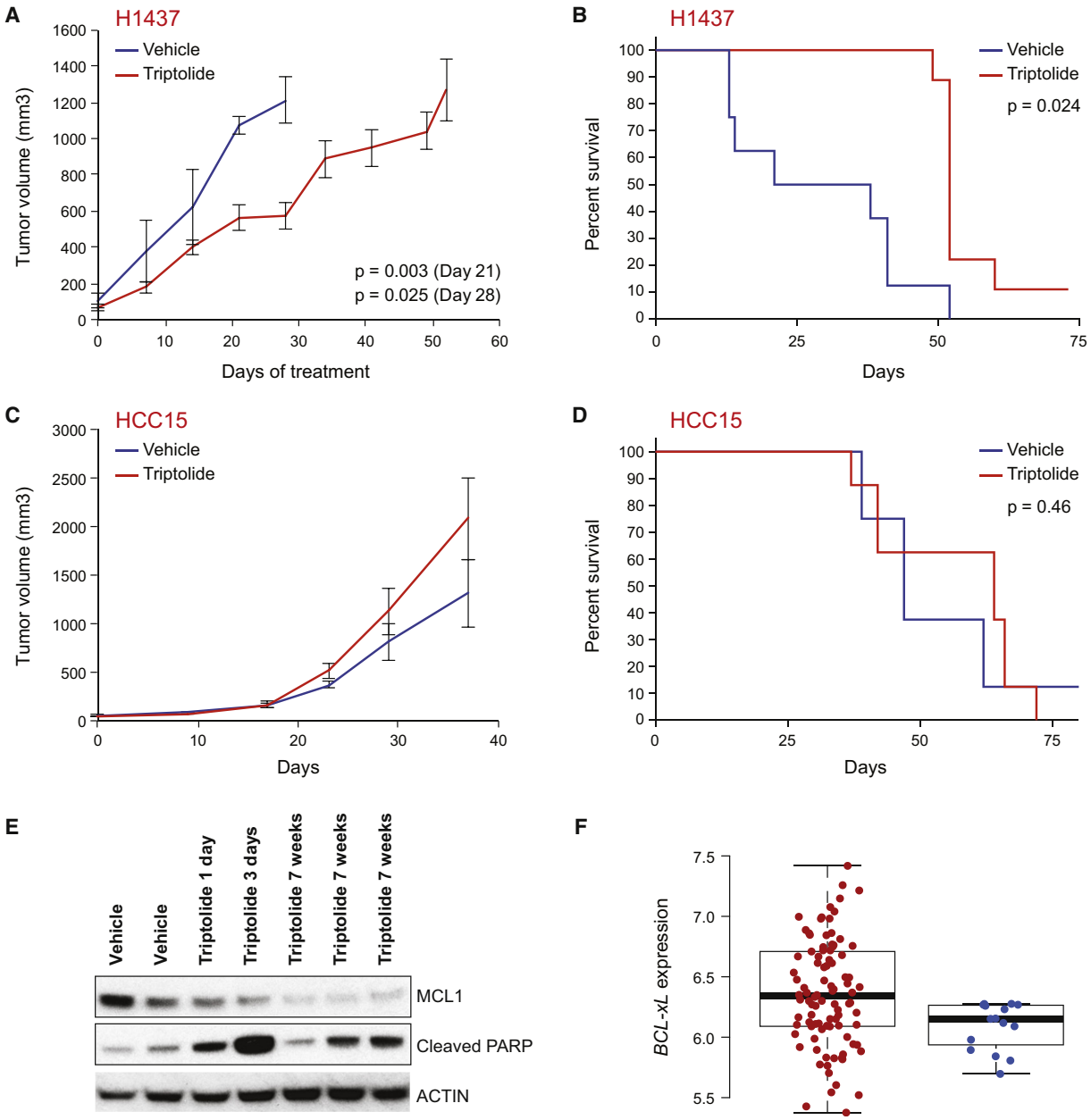

Figure 6. Cells Expressing Low Levels of *BCL-xL* Were Sensitive to Triptolide In Vivo

(A–D) H1437 (low *BCL-xL* expression; A and B) and HCC15 (high *BCL-xL* expression; C and D) NSCLC cell lines were grown as xenografts in NOD-SCID mice, and the mice were treated with triptolide or vehicle as indicated. (A and C) Tumor volume. (B and D) Survival curves. Error bars indicate standard deviation of tumor volume of eight or nine mice.

(E) Triptolide treatment in vivo reduced MCL1 expression and induced PARP cleavage, a marker of apoptosis in tumors. Mice were treated either with vehicle alone or triptolide for 7 weeks, or with vehicle for 7 weeks followed by 1 or 3 days of triptolide.

(F) Correlation between *BCL-xL* expression levels and resistance to epirubicin in ER-negative breast cancer patients (GEO accession number GSE16446). The distribution of *BCL-xL* expression levels, averaged over all *BCL-xL* probe sets on the Affymetrix U133 Plus 2 array, is displayed as a box plot for patients who obtained (n = 16, blue dots, right column) or did not obtain (n = 98, red dots, left column) pathological complete response to single-agent epirubicin treatment. Whiskers of box plots represent 5%–95% data span. Box plots present median, 25th, and 75th percentiles of data.

See also Figure S5.

Matthew Meyerson at the Broad Institute. *Bak*$^{-/-}$, *Bax*$^{-/-}$, and *Bax*$^{-/-}$;*Bak*$^{-/-}$ MEFs were gifts from Anthony Letai at the Dana-Farber Cancer Institute. Caspase activity was measured by the Caspase-Glo 3/7 kit and cell viability was measured by CellTiter-Glo (both from Promega). cDNAs for ectopic expression were from the Human ORFeome Collection by Mark Vidal at the Dana-Farber Cancer Institute. Compounds were purchased from commercial sources listed in Table S2 or were synthesized at the Broad Institute.

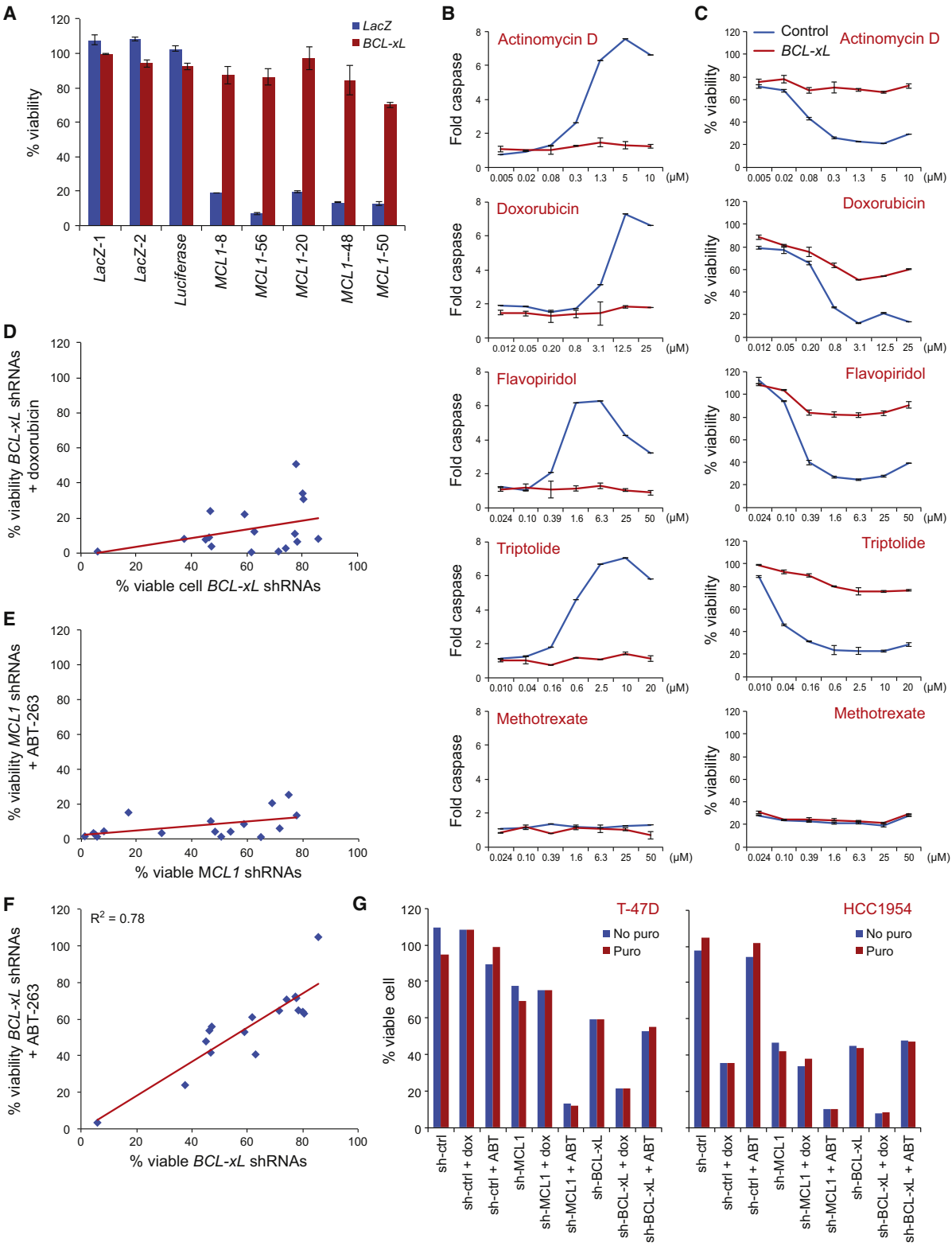

Figure 7. *BCL-xL* Expression Determined Sensitivity to TR Compounds and *MCL1* Repression

(A) Effect of ectopic expression of *BCL-xL* on apoptosis induced by *MCL1* shRNAs in HMC-1-8 cells. Error bars indicate standard deviation of duplicate measurements.

(B and C) Ectopic expression of *BCL-xL* protected sensitive HMC-1-8 cells from TR compounds but not methotrexate, as measured both by caspase activity (B) and cell viability (C). Error bars indicate standard deviation of duplicate measurements.

High-Throughput Gene-Expression Screen for Proximal Apoptosis Genes and Gene-Expression Profiling by Microarray

MCF7 cells growing in 384-well dishes were treated with 2,922 small molecules from small-molecule libraries from the Broad Institute Chemical Biology Program for 8 hr before being lysed. mRNA in cell lysates was hybridized to dT_{20}-conjugated plates (QIAGEN) and then reverse transcribed by Superscript II (Promega). The resulting covalently attached cDNA was amplified by ligation-mediated amplification. For each gene to be assayed, upstream and downstream probes with unique barcode tags and universal primer sites were annealed to targeted cDNA, and ligation by Taq DNA ligase (New England BioLabs) generated a sequence complementary to the transcript. The ligation product was PCR amplified using biotin-conjugated universal primers. The PCR products were then captured by hybridization to probes complementary to the barcodes that were linked to uniquely colored polystyrene beads (Luminex). The products were subsequently stained with streptavidin-phycoerythrin (SAPE) (Invitrogen). Each gene product was identified by the color of its capture bead and quantified using the associated SAPE fluorescence, as measured by a Luminex detector. MCF-7 cells were treated with 500 nM triptolide or 2.5 μM actinomycin D for 2, 4, or 6 hr, and gene expression was profiled using Affymetrix microarrays (Gene Expression Omnibus [GEO] accession number GSE28662).

RNAi and Ectopic Expression

shRNA viral infection was performed as previously described (Moffat et al., 2006). The targeted sequences for the best shRNAs for *MCL1* and *BCL-xL* are listed in Supplemental Experimental Procedures. Cell viability following treatment with *MCL1* or *BCL-xL* shRNAs was compared to results using three control shRNAs against luciferase or LacZ. For combination studies, cells infected with lentivirus carrying shRNAs were selected with or without puromycin (2.5 μg/ml) for 2 days before small molecules were added. Cell viability was measured 24 hr after addition of small molecules. A FLAG tag was added N-terminal of MCL1 or BCL-xL, and FLAG-MCL1 or FLAG-BCL-xL was cloned into an Entry vector (Invitrogen) followed by recombination into a murine stem cell virus (MSCV) destination vector. A *BCL-xL* Entry clone was also cloned into the pLenti6.2 destination vector (Invitrogen) for Figures 7A–7C.

Western Blot and Coimmunoprecipitation

Cells in Figure 6A were lysed in cell lysis buffer (Cell Signaling Technology). Otherwise, cells were lysed in CHAPS lysis buffer (50 mM Tris-Cl [pH 7.4], 150 mM NaCl, 1% CHAPS, 1 mM EDTA, 1 mM EGTA, protease inhibitors, PhosSTOP [Roche], and 20 μM MG132). Protein lysates were incubated with antibody for MCL1 (Santa Cruz Biotechnology) or BCL-xL (Cell Signaling Technology) overnight, and then protein A/G Plus beads (Santa Cruz Biotechnology) were added and incubated for an additional 4 hr. Agarose beads conjugated with an MCL1 antibody and an MCL1 peptide were used in Figure 5D. Anti-FLAG beads and 3X FLAG peptides (both from Sigma) were used in Figure 8E. Antibodies for MCL1 western blots were from Santa Cruz Biotechnology and BD Pharmingen. BCL-xL, BIM, PUMA, BAK, and PARP antibodies were from Cell Signaling Technology. BAX and ACTIN antibodies were from Millipore. Protein quantification was performed with ImageJ (NIH).

Animal Studies

Mice were imaged 2 weeks after subcutaneous injection of H1437-Luc-mCherry or HCC15-Luc-mCherry cells to identify mice with established tumor burden. Tumor measurements were taken twice weekly to track tumor volume. All mice had established tumors at 2 weeks and were entered into treatment groups each containing eight or nine mice, with all groups having around the same bioluminescent imaging average. Treatments were administered daily via intraperitoneal injection and mice were measured weekly for 6 weeks. The animals had tumor measurements taken twice weekly. The time to sacrifice was determined by tumor volume reaching 1,500 cm^2 or tumor ulceration. The xenograft mice were generated, housed, and bred in the Dana-Farber Cancer Institute animal facility. All animal experiments were approved by the Dana-Farber Cancer Institute Institutional Animal Care and Use Committee.

SUPPLEMENTAL INFORMATION

Supplemental Information includes five figures, two tables, and Supplemental Experimental Procedures and can be found with this article online at doi:10.1016/j.ccr.2012.02.028.

ACKNOWLEDGMENTS

This work was supported by NIH grant nos. P01 CA068484 and 5U54CA112962 (to T.R.G.). G.W. was supported by a postdoctoral fellowship from The Damon Runyon Cancer Research Foundation. R.B. was supported by a grant from the Novartis Institutes of Biomedical Research. The authors thank the Broad Institute Chemical Biology Platform for assistance in small-molecule screening; the Broad Institute Genetic Analysis Platform for Affymetrix microarray profiling; the Broad-Novartis Cancer Cell Line Encyclopedia Project for data sharing; Joshua Gould for assistance in data analysis; Jinyan Du, Xiaodong Lu, and Emily Gray for technical assistance; and Leslie Gaffney and Lauren Solomon for editorial assistance.

Received: May 10, 2011
Revised: December 12, 2011
Accepted: February 27, 2012
Published: April 16, 2012

REFERENCES

Adams, J.M., and Cory, S. (2007). The Bcl-2 apoptotic switch in cancer development and therapy. Oncogene *26*, 1324–1337.

Adams, K.W., and Cooper, G.M. (2007). Rapid turnover of mcl-1 couples translation to cell survival and apoptosis. J. Biol. Chem. *282*, 6192–6200.

Basso, K., Margolin, A.A., Stolovitzky, G., Klein, U., Dalla-Favera, R., and Califano, A. (2005). Reverse engineering of regulatory networks in human B cells. Nat. Genet. *37*, 382–390.

Beroukhim, R., Mermel, C.H., Porter, D., Wei, G., Raychaudhuri, S., Donovan, J., Barretina, J., Boehm, J.S., Dobson, J., Urashima, M., et al. (2010). The landscape of somatic copy-number alteration across human cancers. Nature *463*, 899–905.

Bewry, N.N., Nair, R.R., Emmons, M.F., Boulware, D., Pinilla-Ibarz, J., and Hazlehurst, L.A. (2008). Stat3 contributes to resistance toward BCR-ABL inhibitors in a bone marrow microenvironment model of drug resistance. Mol. Cancer Ther. *7*, 3169–3175.

Buggins, A.G., Pepper, C., Patten, P.E., Hewamana, S., Gohil, S., Moorhead, J., Folarin, N., Yallop, D., Thomas, N.S., Mufti, G.J., et al. (2010). Interaction with vascular endothelium enhances survival in primary chronic lymphocytic leukemia cells via NF-κB activation and de novo gene transcription. Cancer Res. *70*, 7523–7533.

Chen, R., Keating, M.J., Gandhi, V., and Plunkett, W. (2005). Transcription inhibition by flavopiridol: mechanism of chronic lymphocytic leukemia cell death. Blood *106*, 2513–2519.

Chen, S., Dai, Y., Harada, H., Dent, P., and Grant, S. (2007). Mcl-1 down-regulation potentiates ABT-737 lethality by cooperatively inducing Bak activation and Bax translocation. Cancer Res. *67*, 782–791.

Danial, N.N., and Korsmeyer, S.J. (2004). Cell death: critical control points. Cell *116*, 205–219.

(D–F) The effects of *BCL-xL* shRNAs (D and F) or *MCL1* shRNAs (E) on cell viability plotted on the x axis against sensitivity to the combination of *BCL-xL* shRNAs (D and F) or *MCL1* shRNAs (E) and doxorubicin (D) or ABT-263 (E and F) in 17 breast cancer cell lines. Cells were infected with viruses carrying shRNAs for *MCL1* or *BCL-xL* for 3 days, or 2 days followed by treatment with 5 μM doxorubicin or 1 μM ABT-263 for an additional 24 hr (median of five *MCL1* shRNAs or *BCL-xL* shRNAs, as indicated).
(G) Examples of combination treatment of *MCL1* or *BCL-xL* shRNAs and doxorubicin (dox) or ABT-263 (ABT). Puro, puromycin.
See also Figure S5.

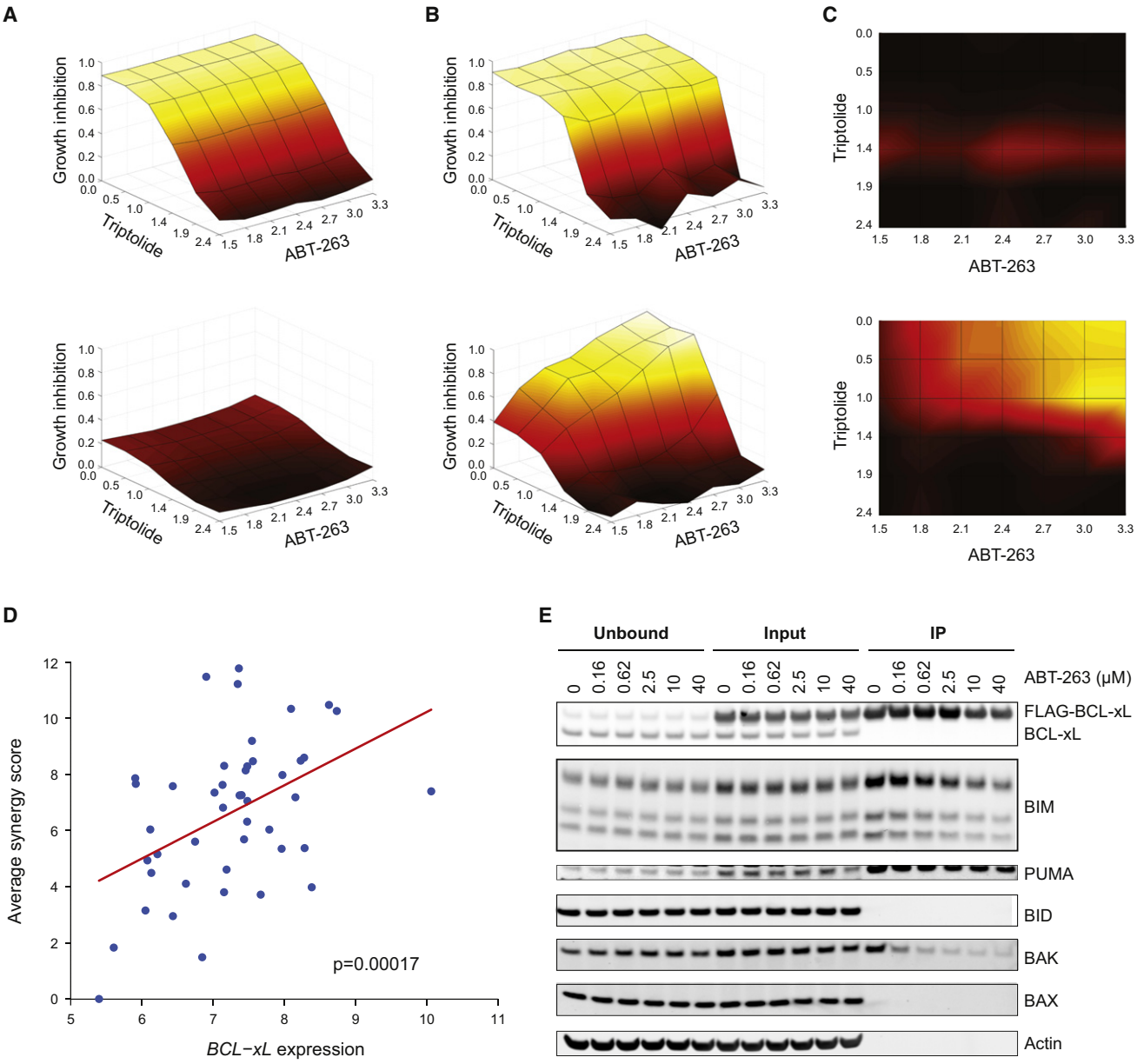

Figure 8. TR Compounds and BCL-xL Inhibitor Compounds Synergistically Killed Cells with High *BCL-xL* Expression

(A–C) Example of synergy calculation. Cell lines expressing *BCL-xL* at the lowest (NCI-H23; top panel) and highest (SKLU1; bottom panel) levels, across a panel of 74 NSCLC cell lines.

(A) Bliss independence model. Dose-response curves for single-agent treatment with ABT-263 and triptolide were used to compute the null-hypothesis surface of expected response to combination treatment with ABT-263 and triptolide using a Bliss independence model. The x and y axes represent concentrations of ABT-263 and triptolide in log10(nM), and the z axis (as well as the color scale) represents the expected percent growth inhibition for each combination of compound concentrations under the null-hypothesis model.

(B) Dose-response matrix. Observed response surfaces for the combination experiments were plotted.

(C) Excess over Bliss independence. Excess percent growth inhibition over the null-hypothesis model was computed for each combination of compound concentrations by subtracting the growth inhibition values displayed in (A) from those in (B). Black represents no excess growth inhibition and yellow represents excess growth inhibition (scale 0–1).

(D) *BCL-xL* expression level versus compound synergy across the panel of 74 cell lines. The x axis displays the log2 expression level of *BCL-xL*. The y axis displays the synergy score, computed by summing the excess over Bliss independence values (as shown in C) over all combinations of compound concentrations. The synergy scores displayed in the plot represent the average synergy score over the four combination experiments, performed by pairing triptolide or actinomycin D with ABT-263 or ABT-737.

(E) Cells stably expressing FLAG-tagged BCL-xL were treated with ABT-263 at the indicated concentrations for 3 hr, subjected to immunoprecipitation with anti-FLAG antibody beads, and eluted with 3X FLAG peptides. The IP fraction was 5-fold more concentrated than input and unbound.

Desmedt, C., Di Leo, A., de Azambuja, E., Larsimont, D., Haibe-Kains, B., Selleslags, J., Delaloge, S., Duhem, C., Kains, J.P., Carly, B., et al. (2011). Multifactorial approach to predicting resistance to anthracyclines. J. Clin. Oncol. *29*, 1578–1586.

Gomez-Bougie, P., Wuillème-Toumi, S., Ménoret, E., Trichet, V., Robillard, N., Philippe, M., Bataille, R., and Amiot, M. (2007). Noxa up-regulation and Mcl-1 cleavage are associated to apoptosis induction by bortezomib in multiple myeloma. Cancer Res. *67*, 5418–5424.

Gong, Y., Somwar, R., Politi, K., Balak, M., Chmielecki, J., Jiang, X., and Pao, W. (2007). Induction of BIM is essential for apoptosis triggered by EGFR kinase inhibitors in mutant EGFR-dependent lung adenocarcinomas. PLoS Med. *4*, e294.

Hanahan, D., and Weinberg, R.A. (2011). Hallmarks of cancer: the next generation. Cell *144*, 646–674.

Hieronymus, H., Lamb, J., Ross, K.N., Peng, X.P., Clement, C., Rodina, A., Nieto, M., Du, J., Stegmaier, K., Raj, S.M., et al. (2006). Gene expression signature-based chemical genomic prediction identifies a novel class of HSP90 pathway modulators. Cancer Cell *10*, 321–330.

Jeffers, J.R., Parganas, E., Lee, Y., Yang, C., Wang, J., Brennan, J., MacLean, K.H., Han, J., Chittenden, T., Ihle, J.N., et al. (2003). Puma is an essential mediator of p53-dependent and -independent apoptotic pathways. Cancer Cell *4*, 321–328.

Keuling, A.M., Felton, K.E., Parker, A.A., Akbari, M., Andrew, S.E., and Tron, V.A. (2009). RNA silencing of Mcl-1 enhances ABT-737-mediated apoptosis in melanoma: role for a caspase-8-dependent pathway. PLoS One *4*, e6651.

Krajewska, M., Fenoglio-Preiser, C.M., Krajewski, S., Song, K., Macdonald, J.S., Stemmerman, G., and Reed, J.C. (1996a). Immunohistochemical analysis of Bcl-2 family proteins in adenocarcinomas of the stomach. Am. J. Pathol. *149*, 1449–1457.

Krajewska, M., Krajewski, S., Epstein, J.I., Shabaik, A., Sauvageot, J., Song, K., Kitada, S., and Reed, J.C. (1996b). Immunohistochemical analysis of bcl-2, bax, bcl-X, and mcl-1 expression in prostate cancers. Am. J. Pathol. *148*, 1567–1576.

Kuroda, J., Puthalakath, H., Cragg, M.S., Kelly, P.N., Bouillet, P., Huang, D.C., Kimura, S., Ottmann, O.G., Druker, B.J., Villunger, A., et al. (2006). Bim and Bad mediate imatinib-induced killing of Bcr/Abl^{+} leukemic cells, and resistance due to their loss is overcome by a BH3 mimetic. Proc. Natl. Acad. Sci. USA *103*, 14907–14912.

Lamb, J., Crawford, E.D., Peck, D., Modell, J.W., Blat, I.C., Wrobel, M.J., Lerner, J., Brunet, J.P., Subramanian, A., Ross, K.N., et al. (2006). The Connectivity Map: using gene-expression signatures to connect small molecules, genes, and disease. Science *313*, 1929–1935.

Lee, S.I., Dudley, A.M., Drubin, D., Silver, P.A., Krogan, N.J., Pe'er, D., and Koller, D. (2009). Learning a prior on regulatory potential from eQTL data. PLoS Genet. *5*, e1000358.

Leuenroth, S.J., and Crews, C.M. (2008). Triptolide-induced transcriptional arrest is associated with changes in nuclear substructure. Cancer Res. *68*, 5257–5266.

Lin, X., Morgan-Lappe, S., Huang, X., Li, L., Zakula, D.M., Vernetti, L.A., Fesik, S.W., and Shen, Y. (2007). 'Seed' analysis of off-target siRNAs reveals an essential role of Mcl-1 in resistance to the small-molecule Bcl-2/Bcl-XL inhibitor ABT-737. Oncogene *26*, 3972–3979.

Lindsten, T., Ross, A.J., King, A., Zong, W.X., Rathmell, J.C., Shiels, H.A., Ulrich, E., Waymire, K.G., Mahar, P., Frauwirth, K., et al. (2000). The combined functions of proapoptotic Bcl-2 family members bak and bax are essential for normal development of multiple tissues. Mol. Cell *6*, 1389–1399.

Margolin, A.A., Nemenman, I., Basso, K., Wiggins, C., Stolovitzky, G., Dalla Favera, R., and Califano, A. (2006). ARACNE: an algorithm for the reconstruction of gene regulatory networks in a mammalian cellular context. BMC Bioinformatics *7* (*Suppl 1*), S7.

Martin, M., Romero, A., Cheang, M.C.U., López García-Asenjo, J.A., García-Saenz, J.A., Oliva, B., Román, J.M., He, X., Casado, A., de la Torre, J., et al. (2011). Genomic predictors of response to doxorubicin versus docetaxel in primary breast cancer. Breast Cancer Res. Treat. *128*, 127–136.

Mérino, D., Strasser, A., and Bouillet, P. (2011). Bim must be able to engage all pro-survival Bcl-2 family members for efficient tumor suppression. Oncogene, in press. Published online November 14, 2011. 10.1038/onc.2011.508.

Moffat, J., Grueneberg, D.A., Yang, X., Kim, S.Y., Kloepfer, A.M., Hinkle, G., Piqani, B., Eisenhaure, T.M., Luo, B., Grenier, J.K., et al. (2006). A lentiviral RNAi library for human and mouse genes applied to an arrayed viral high-content screen. Cell *124*, 1283–1298.

Moretti, E., Oakman, C., and Di Leo, A. (2009). Predicting anthracycline benefit: have we made any progress? Curr. Opin. Oncol. *21*, 507–515.

Oltersdorf, T., Elmore, S.W., Shoemaker, A.R., Armstrong, R.C., Augeri, D.J., Belli, B.A., Bruncko, M., Deckwerth, T.L., Dinges, J., Hajduk, P.J., et al. (2005). An inhibitor of Bcl-2 family proteins induces regression of solid tumours. Nature *435*, 677–681.

Peck, D., Crawford, E.D., Ross, K.N., Stegmaier, K., Golub, T.R., and Lamb, J. (2006). A method for high-throughput gene expression signature analysis. Genome Biol. *7*, R61.

Petros, A.M., Olejniczak, E.T., and Fesik, S.W. (2004). Structural biology of the Bcl-2 family of proteins. Biochim. Biophys. Acta *1644*, 83–94.

Rossi, C., Gasparini, G., Canobbio, L., Galligioni, E., Volpe, R., Candiani, E., Toffoli, G., and D'Incalci, M. (1987). Doxorubicin distribution in human breast cancer. Cancer Treat. Rep. *71*, 1221–1226.

Stewart, M.L., Fire, E., Keating, A.E., and Walensky, L.D. (2010). The MCL-1 BH3 helix is an exclusive MCL-1 inhibitor and apoptosis sensitizer. Nat. Chem. Biol. *6*, 595–601.

Tewey, K.M., Rowe, T.C., Yang, L., Halligan, B.D., and Liu, L.F. (1984). Adriamycin-induced DNA damage mediated by mammalian DNA topoisomerase II. Science *226*, 466–468.

Titov, D.V., Gilman, B., He, Q.L., Bhat, S., Low, W.K., Dang, Y., Smeaton, M., Demain, A.L., Miller, P.S., Kugel, J.F., et al. (2011). XPB, a subunit of TFIIH, is a target of the natural product triptolide. Nat. Chem. Biol. *7*, 182–188.

Tse, C., Shoemaker, A.R., Adickes, J., Anderson, M.G., Chen, J., Jin, S., Johnson, E.F., Marsh, K.C., Mitten, M.J., Nimmer, P., et al. (2008). ABT-263: a potent and orally bioavailable Bcl-2 family inhibitor. Cancer Res. *68*, 3421–3428.

van Delft, M.F., Wei, A.H., Mason, K.D., Vandenberg, C.J., Chen, L., Czabotar, P.E., Willis, S.N., Scott, C.L., Day, C.L., Cory, S., et al. (2006). The BH3 mimetic ABT-737 targets selective Bcl-2 proteins and efficiently induces apoptosis via Bak/Bax if Mcl-1 is neutralized. Cancer Cell *10*, 389–399.

Villunger, A., Michalak, E.M., Coultas, L., Müllauer, F., Böck, G., Ausserlechner, M.J., Adams, J.M., and Strasser, A. (2003). p53- and drug-induced apoptotic responses mediated by BH3-only proteins puma and noxa. Science *302*, 1036–1038.

Voortman, J., Checinska, A., Giaccone, G., Rodriguez, J.A., and Kruyt, F.A. (2007). Bortezomib, but not cisplatin, induces mitochondria-dependent apoptosis accompanied by up-regulation of noxa in the non-small cell lung cancer cell line NCI-H460. Mol. Cancer Ther. *6*, 1046–1053.

Warr, M.R., and Shore, G.C. (2008). Unique biology of Mcl-1: therapeutic opportunities in cancer. Curr. Mol. Med. *8*, 138–147.

Wei, G., Twomey, D., Lamb, J., Schlis, K., Agarwal, J., Stam, R.W., Opferman, J.T., Sallan, S.E., den Boer, M.L., Pieters, R., et al. (2006). Gene expression-based chemical genomics identifies rapamycin as a modulator of MCL1 and glucocorticoid resistance. Cancer Cell *10*, 331–342.

Wei, M.C., Zong, W.X., Cheng, E.H., Lindsten, T., Panoutsakopoulou, V., Ross, A.J., Roth, K.A., MacGregor, G.R., Thompson, C.B., and Korsmeyer, S.J. (2001). Proapoptotic BAX and BAK: a requisite gateway to mitochondrial dysfunction and death. Science *292*, 727–730.

Wiegmans, A.P., Alsop, A.E., Bots, M., Cluse, L.A., Williams, S.P., Banks, K.M., Ralli, R., Scott, C.L., Frenzel, A., Villunger, A., and Johnstone, R.W. (2011). Deciphering the molecular events necessary for synergistic tumor cell apoptosis mediated by the histone deacetylase inhibitor vorinostat and the BH3 mimetic ABT-737. Cancer Res. *71*, 3603–3615.

Zhou, P., Levy, N.B., Xie, H., Qian, L., Lee, C.Y., Gascoyne, R.D., and Craig, R.W. (2001). MCL1 transgenic mice exhibit a high incidence of B-cell lymphoma manifested as a spectrum of histologic subtypes. Blood *97*, 3902–3909.